Comparison of Second-Generation Stents for Application in the Superficial Femoral Artery: An In Vitro Evaluation Focusing on Stent Design

Müller-Hülsbeck S, Schäfer PJ, Charalambous N,
Yagi H, Heller M, Jahnke T

◆ EXPERIMENTAL INVESTIGATION ────────────────────────── ◆

Comparison of Second-Generation Stents for Application in the Superficial Femoral Artery:
An In Vitro Evaluation Focusing on Stent Design

Stefan Müller-Hülsbeck, MD[1]**; Philipp J. Schäfer, MD**[2]**; Nikolas Charalambous, MD**[2]**; Hiroshi Yagi**[3]**; Martin Heller, MD**[2]**; and Thomas Jahnke, MD**[2]

[1]Department of Diagnostic and Interventional Radiology/Neuroradiology, Academic Hospitals Flensburg, Germany. [2]Department of Radiology, University Hospitals Schleswig-Holstein – Campus Kiel, Germany. [3]Terumo, Tokyo, Japan.

◆ ──────────────────────────────────── ◆

Purpose: To examine and compare in an ex vivo study different nitinol stent designs intended for the superficial femoral artery (SFA) with regard to the appearance of fracture.
Methods: Seven different 8-×40-mm nitinol stents were evaluated (Misago, Absolute, Smart, Luminexx, Sentinol, Lifestent NT, and Sinus-Superflex). Finite element analysis (FEA) was used for digitalized stent design comparison; the strain during stent movement was calculated for bending, compression, and torsion. Additional mechanical fatigue tests for bending (70°), compression (40%), and torsion (twisted counterclockwise by 180°) were performed up to 650,000 cycles or until a fracture was observed.
Results: The FEA bending test showed that only the Misago, LifeStent, and Absolute stents presented no zones of high strain; in the torsion test, the Smart stent also had no zones of high strain. Macroscopic evaluation after mechanical bending indicated that the LifeStent performed the best (no stent fracture after 650,000 cycles). Misago and Absolute stents showed fractures at 536,000 cycles and 456,667 cycles, respectively (range 320,000–650,000 cycles). After compression and torsion testing, Misago showed no stent fracture after 650,000 cycles. The worst performing stent was Luminexx during all test cycles.
Conclusion: The 7 SFA stents showed differences in the incidence of high strain zones, which indicates a potential for stent fracture, as demonstrated by the mechanical fatigue tests. Differences in stent design might play a major role in the appearance of stent strut fracture related to restenosis and reocclusion.

J Endovasc Ther. 2010;17:767–776

Key words: superficial femoral artery, stent, nitinol, experimental study, finite element analysis, stent design, fatigue testing, stent fracture, compression, bending, torsion

◆ ──────────────────────────────────── ◆

Endovascular stenting is a rapidly evolving technology for treatment of either arterial or venous obstruction, as well aneurysmal disease, in the circulatory system. Several clinical reports and trials evaluated the effect of stents in the superficial femoral artery (SFA).

In this dedicated segment, balloon-expandable stents were not superior to balloon angioplasty alone,[1] and self-expanding stents failed to show a beneficial effect in short lesions <5 cm in length.[2] For longer lesions, trials report a benefit for stents compared to

balloon angioplasty alone.[3] In particular, this latter data has opened the door to a more liberal and widespread use of stents in the SFA. Unfortunately, with longer stented segments, the incidence of stent fractures appears to rise, though the reported fracture rates for today's commercially available designs differ widely from 1.8% to 18%.[4–8] Even if clinically relevant complications of stent fractures rarely occur (other than restenosis or reocclusion), it is important to gather more information about the potential risk of stent fracture. In addition to clinical data, theoretical and experimental studies are needed prior to the release of new products.

The optimization of material property, surface finish, and stent design are necessary for the development of a durable stent. Many self-expanding stents share the same basic construction: the stents are laser-cut from a nickel-titanium alloy tube, and the surface of the stent is electropolished to make it smooth and corrosion-resistant. However, the stent design is quite variable among products and may play a significant role in the durability of the stent. It is expected that an optimal stent design could reduce the potential risk of a stent fracture. Therefore, we used two methods of analysis, finite element analysis (FEA) and mechanical fatigue testing, to identify the potential fracture risks of some currently available SFA stent designs.

METHODS

Seven different nitinol stents measuring 8-×40-mm were evaluated: Misago (Terumo, Tokyo, Japan), Absolute (Abbott Vascular, Santa Clara, CA, USA), Smart (Cordis Endovascular, Miami Lakes, FL, USA), Luminexx (C.R. Bard, Tempe, AZ, USA), Sentinol (Boston Scientific, Natick, MA, USA), Lifestent NT (C.R. Bard), and Sinus-Superflex (Optimed, Ettlingen, Germany). At least one sample from each manufacturer was tested (Table 1).

Stent Design

The basic stent design consisted of a repeating pattern of zigzag units linked together. The geometry of the zigzag or peak-to-valley design differed among models, as well as the bridges or transition zones connecting the zigzag elements. The cell size depended on the number of parallel peak-to-valley areas and the number of connections; fewer bridges between zigzags made the stent design more open and flexible.

Misago's zigzags were not straight; they included a short segment that included 2 large angled bridges located in the center of a zigzag to serve as a transition zone to the next zigzag and cell area, respectively. The zigzag design of the Absolute stent was very similar: straight bridges from one peak to another peak parallel to the stent axis connected the zigzags.

The zigzags and short peak-to-valley bridges of the Smart stent were in a slightly elongated S-shaped curve not parallel to the stent axis. The Luminexx stent had a zigzag design that was similar to that of the Smart stent, but the peaks and valleys were connected directly without any bridges. Sentinol also had short peak-to-valley bridges, with zigzags similar to the Smart and Luminexx stents. Lifestent was quite similar in terms of design to the Smart stent. Sinus-Superflex consisted of elongated zigzag elements with an additional elongation in the mid part of a zigzag element; short peak-to-valley bridges orientated vertical to the stent axis connected the zigzags.

Finite Element Analysis

FEA is a method of finding approximate solutions to partial differential equations and integral equations. In this stent comparison, digitized models of the stent designs were analyzed, and the strains during stent movement were calculated according to the 3-dimensional (3D) solid element and hexahedral 8-node element method (ADINA ver. 8.5; ADINA R&D, Watertown, MA, USA). To keep the analysis runtime reasonable, a finite-element mesh consisting of 3 elements in the stent strut width direction and 2 elements in the stent wall thickness direction was used. The material properties of each stent design were obtained from strain-stress curves of dog bone–shaped samples produced by manufacturing processes equivalent to the stent (laser-cut, heat set, electropolish). These

TABLE 1
High Strain Zones During Finite Element Analysis of Bending, Compression,
and Torsion for the 7 Nitinol Stents

	Design	Numbers Tested	Bending	Compression	Torsion
Misago	Open cell zigzag units, and the center of the zigzags are connected with 2 large angled bridges	15	— (n=5)	— (n=5)	— (n=5)
Absolute	Open cell zigzag; peak-to-peak connected with straight bridges	7	— (n=3)	— (n=3)	— (n=1)
Smart	Open cell zigzag; peak-to-valley connected with S-shaped bridge	7	++ (n=3)	++ (n=3)	— (n=1)
Luminexx	Open cell zigzag; peak-to-valley connected directly	7	++ (n=3)	++ (n=3)	++ (n=1)
Sentinol	Open cell zigzag; peak-to-valley connected with short straight bridge	3	++ (n=1)	++ (n=1)	++ (n=1)
LifeStent	Open cell zigzag; similar to Smart	1/1/1	+ (n=1)	— (n=1)	— (n=1)
Sinus-SuperFlex	Open cell zigzag; peak-to-valley connected with short bridges	1/1/1	+ (n=1)	++ (n=1)	++ (n=1)

Stents with no red (strain) zones as defined in the text were indicated by a ''−'', stents with <10 red zones were given a ''+'', and stents with ≥10 red zones were counted as ''++''.

material data were applied for all involved stent samples so the analysis accurately represented the differences in the fracture-resistant characteristics associated with the stent design. The nitinol material properties and the surface finish were ignored, as the alloy was the same for all stents.

For bending, the stent was fixed at 15 mm from the proximal edge and the distal edge was pressed down by 12 mm. To evaluate compression, one end of the stent was fixed and the other end was compressed along the long axis of the stent until the length became 20% shorter than the original length. Finally, for torsion, one end of the stent was fixed and the other end was twisted counterclockwise by 60°. The strain that the stent received under each of these conditions was calculated; high strain zones (~0.9% strain or more) appeared in red on the simulations. For semi-quantitative evaluation, red zones greater than a stent strut thickness were counted as one high strain area. Stents with no red zones as defined above were indicated by a ''−'',

stents with <10 red zones were given a ''+'', and stents with ≥10 red zones were marked as ''++''.

Mechanical Fatigue Testing

All tests were done in a regulated atmosphere at 37°C on actual 8-×40-mm stents. Each test described below was repeated up to a maximum of 650,000 cycles. The occurrence of the stent fracture was checked at 1,000, 5,000, 10,000, 15,000, 20,000 and 25,000 cycles, then every 10,000 cycles from 30,000 to 100,000 and every 20,000 cycles from 100,000 to the 650,000 maximum. The test was continued until a fracture was observed or the maximum was reached.

Bending. The center point of the stent sample was placed between two 6-mm-thick supports spaced 6 mm apart. The proximal end of the stent was fixed, and the distal end at 15 mm from the center point was flexed downward by 40° and flexed upward by 30° (Fig. 1).
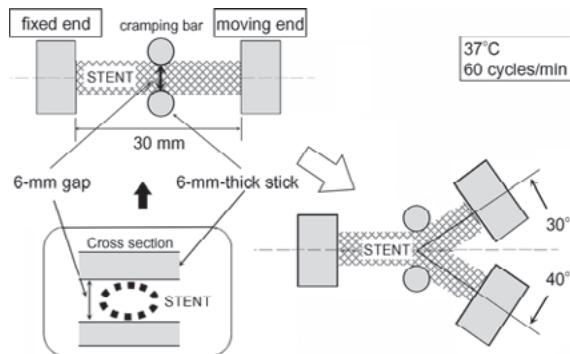
Figure 1 ◆ Schematic of the setup for the bending test.

Compression. The proximal end of the stent sample was fixed; the other end was compressed along the long axis of the stent until the overall stent length was 40% shorter than the original length and then returned to the original position (Fig. 2).

Torsion. The proximal end of the stent sample was fixed and the other end was twisted counterclockwise by 90° and then twisted clockwise by 180° (90° from the original position; Fig. 3).

Statistical Analysis

The data is presented as mean and range; due to the small sample sizes, no statistical evaluation was performed.
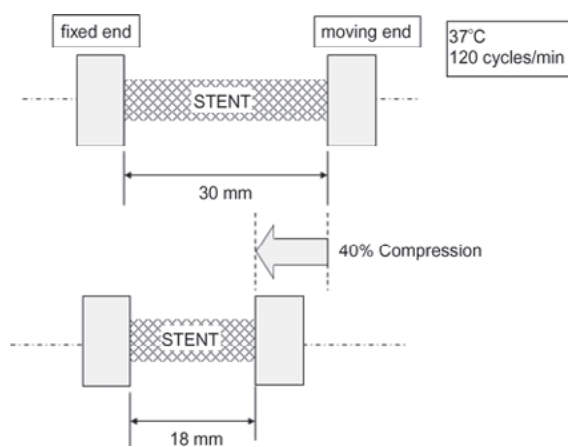

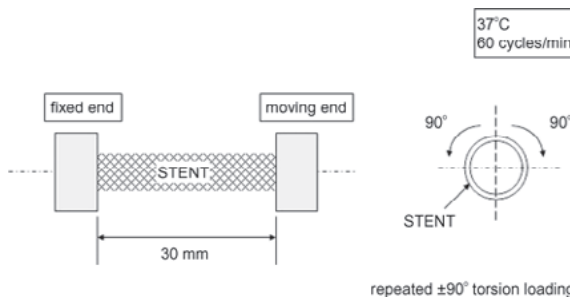**Figure 2** ◆ Schematic of the setup for the compression test.

Figure 3 ◆ Schematic of the setup for the torsion test.

RESULTS

Finite Element Analysis

In the bending tests (Table 1 and Fig. 4A), Misago and Absolute presented no zones of high strain. LifeStent and Sinus-Superflex had <10 zones of high strain during bending. Sentinol (Fig. 4D), Smart (Fig. 4E), and Luminexx (Fig. 4F) had ≥10 high strain areas. In the compression test (Fig. 4B), Misago, Absolute, and LifeStent presented no zones of high strain. Sinus-Superflex had <10 zones of high strain during bending, while Smart, Sentinol, and Luminexx showed ≥10 high strain areas. In the torsion tests (Fig. 4C), Misago, Absolute, Smart, and LifeStent demonstrated no zones of high strain, while Sentinol, Sinus-Superflex, and Luminexx showed ≥10 high strain areas.

Fatigue Testing

In the mechanical bending tests (Table 2), macroscopic evaluation of the LifeStent showed no stent fracture after 650,000 cycles (only 1 sample tested). One of 5 Misago stent samples showed fracture after a mean 536,000 cycles (range 80,000–650,000); 4 samples had no fracture at 650,000 cycles. The Absolute stent had fractures at a mean 456,667 cycles (range 320,000–650,000). Fractures appeared much earlier in the Luminexx stent (mean 2,415 cycles, range 2,000–3,000), Sinus-Superflex (at 5,000 cycles), Sentinol (mean 16,400 cycles, range 8,200–25,000), and Smart (mean 41,667 cycles, range 25,000–50,000).

In the compression tests, macroscopic evaluation of Misago showed no stent frac-

ture after 650,000 cycles (5 samples tested). Again, fractures appeared earlier with Luminexx (mean 1,000 cycles; all 3 samples with fractures), Smart (mean 3,182 cycles, range 2,000–4,545), Sinus-Superflex (4,445 cycles), Sentinol (mean 6,515 cycles, range 4,545–10,000), Absolute (mean 23,333 cycles, range 10,000–40,000), and LifeStent (48,995 cycles).

In the torsion tests, macroscopic evaluation of Misago showed no stent fracture after 650,000 cycles (5 samples tested), while fractures appeared earlier in the individual samples of Luminexx (1,000 cycles), Sinus-Superflex (5,000 cycles), Smart (10,000 cycles), Absolute (60,000 cycles), Sentinol (60,000 cycles), and LifeStent (60,000 cycles).

DISCUSSION

The poor performance of early SFA stents and the complexity of the SFA have prompted the development of new stent designs, so-called second-generation SFA stents. With these dedicated SFA stent designs, stent fracture should no longer be an issue. The latest data indicated low fracture rates $<5\%$ during 6 months of follow-up.[3,7] Potential reasons for stents fractures have been put forth in several clinical evaluations that demonstrated changes of the SFA during leg movement. Computerized fluoroscopy image evaluation of changes in the femoropopliteal segment between the straight-leg (SL) and crossed-leg (CL) positions demonstrated significant changes in length, curvature, and rotation in the popliteal artery and significant but more modest changes in length and rotation in the SFA during movement from the SL to the CL position. The data showed mean shortening of 6.1% and 15.8%, respectively, for the SFA and popliteal artery. The mean rotation angles for the SFA and popliteal artery were $45.6°\pm27.9°$ and $61.1°\pm31.9°$, respectively, and the mean flexion angles were $20.1°\pm1.7°$ and $20.2°\pm14.8°$, respectively. The authors concluded that these data had important implications for endovascular therapies in the femoropopliteal segment.

In other studies, Cheng et al.[10] examined healthy young gymnasts and found the mean shortening of the SFA was 13%±11% and a mean rotation angle of $60°\pm34°$ between the supine and fetal positions. A study of older subjects showed mean shortening values of 5.9%±3.0%, 6.7%±2.1%, and 8.1%±2.0% in the top, middle, and bottom of the SFA, respectively.[11] The mean values of these parameters are reasonable benchmark conditions for testing. However, these data are based on the non-stented vessel; the investigator should consider the post-implant morphological changes in establishing appropriate boundary conditions.

The need for compression analysis was demonstrated by the assessment of magnetic resonance angiography (MRA) datasets of femoropopliteal compression during isometric thigh contraction.[12] A 3D balanced steady-state free precession sequence was used to image a 15- to 20-cm segment of the vasculature during relaxation and voluntary isometric thigh contraction. MRA of the femoropopliteal segment during thigh contraction demonstrated focal compression of the arterial segment in the distal adductor canal region, which may also help explain the high stent failure rate and the high likelihood of atherosclerotic disease in the adductor canal.

In our study, the main focus was on comparing the performance limit to the appearance of fracture for each stent design, so more aggressive boundary conditions were applied. In current mechanical fatigue tests, walking is generally considered a fatigue cycle condition; 10 million cycles simulates 10 years of walking. The fatigue cycles for more severe motion, such as sitting and stair climbing, are not standardized, but there are assumptive calculations[13] on which we based our fatigue testing: sitting = (365 d/y)×(12 h/d)×(60 min/h)×(1 cycle/15 minutes)×10 years = 175,200 cycles; stair climbing = (365 d/y)×(8 flights/d)×(32 stairs/flight)×1 cycle/2 stairs)×10 years = 467,200 cycles. For 10 years, the total for sitting and stair climbing is 642,400 cycles, so the maximum in our study was 650,000 cycles.

As shown in the DURABILITY trial, stent fracture rates may be operator dependent, i.e., a stent implanted in an elongated manner ($\geq$10% over the nominal length) is more likely to develop fractures.[14] However, the long-term clinical significance of the fractures remains unknown, but it is obvious that as
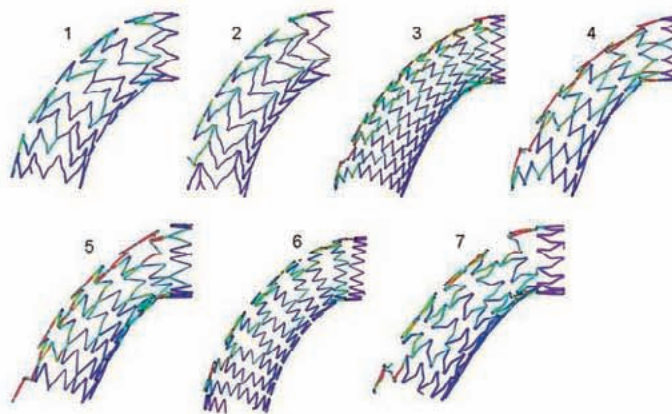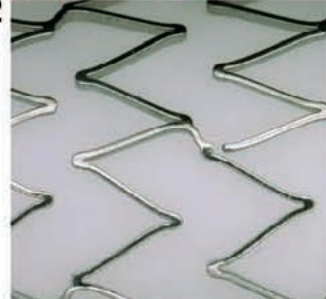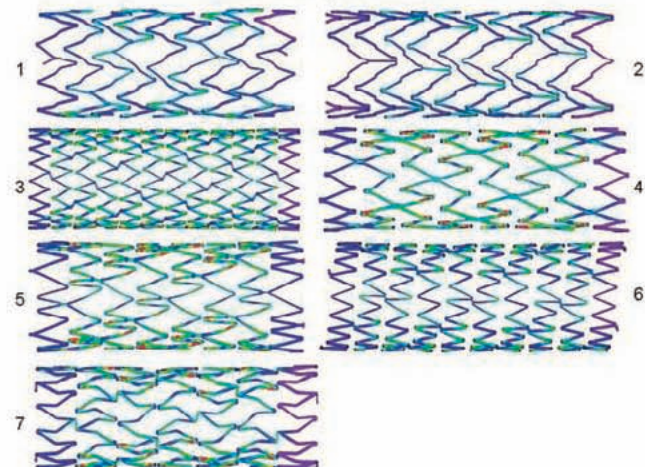
TABLE 2
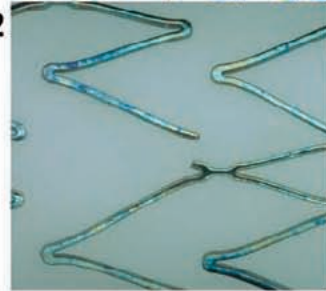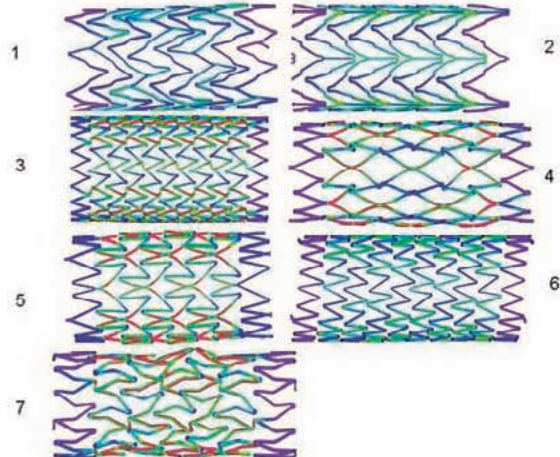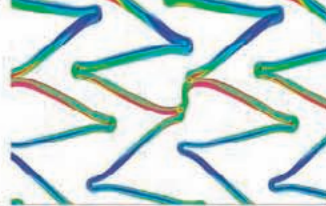Mean Cycles to Stent Fracture During Mechanical Bending, Compression, and Torsion Testing

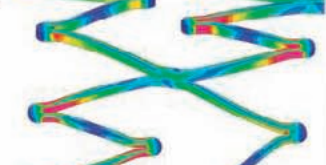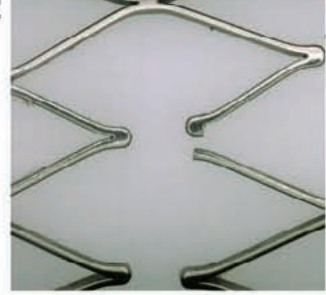|	Numbers Tested: Bending/ Compression/ Torsion	Bending	Compression	Torsion
Misago	5/5/5	536,000	650,000*	650,000*
Absolute	3/3/1	456,667	23,333	60,000
Smart	3/3/1	41,667	3,182	10,000
Luminexx	3/3/1	2,415	1,000	1,000
Sentinol	3/3/1	16,400	6,515	60,000
LifeStent	1/1/1	650,000*	48,995	60,000
Sinus-SuperFlex	1/1/1	5,000	4,445	5,000

* Not broken at 650,000 cycles.

the grade of the fracture worsens, from single strut fracture to multiple fractures and finally loss of stent integrity, the incidences of >50% restenosis and occlusion may rise.

The progression of stent fracture is supposed to be a dynamic process that may become symptomatic in a case of complete transverse linear fracture. As the SFA traverses the adductor canal, a particularly complex combination of forces comes into play, in particular, external compression, torsion, elongation, and flexion. These forces, together with manufacturing processes, will be responsible for stent failure. Any potential stent fracture would have tremendous implications to the patient because stent platforms are so integral to cardiovascular treatment; clinicians and industry, therefore, have an obligation to look for stent refinements. Unfortunately, there is little standardization in the processing, laser cutting, etching,

electropolishing, surface finishing, and fatigue testing of nitinol stents. Because of this, we attempted to gather more information about the influence of stent design on bending, compression, and torsion, as evaluated during FEA and mechanical fatigue tests. Physicians currently have no other way to gather more information about stents and their potential behavior in terms of strut fracture. In order to obtain this missing information to complement clinical data obtained after stent implantation, identical methods for ex vivo testing would be helpful.

Nikanorov et al.[15] also used in vitro fatigue testing to characterize the types and ranges of stent distortion theoretically produced by extremity movement; they used these ranges as parameters for in vitro long-term fatigue testing of commercially available self-expanding nitinol stents. They placed stents (Protégé EverFlex, Smart, Luminexx, LifeStent, Xceed,

←

Figure 4 ◆ Finite element analyses of all stents during (**A**) bending, (**B**) compression, and (**C**) torsion. Legend: 1: Misago, 2: Absolute, 3: Smart, 4: Luminexx, 5: Sentinol, 6: Lifestent NT, and 7: Sinus-Superflex. (**D1**) Finite element analysis of the Sentinol stent during bending, indicating a high strain zone at the zigzags adjacent to the short bridges, which show no high strain areas. (**D2**) Photograph of a fracture in the corresponding stent area. (**D3**) The strut fracture cannot be seen on magnified high-resolution fluoroscopy. (**E1**) Finite element analysis of the Smart stent during bending, indicating high strain zones at the zigzags adjacent to the short S-shaped bridges, which show no high strain areas. (**E2**) Photograph of a fracture in the corresponding stent area. (**E3**) The strut fracture cannot be seen on magnified high-resolution fluoroscopy. (**F1**) Finite element analysis of the Luminexx stent during bending, indicating high strain zones at the zigzags' peaks and valley. (**F2**) Photograph of a fracture in the corresponding stent area. (**F3**) The strut fracture cannot be seen on magnified high-resolution fluoroscopy.

and Absolute) in the SFA of cadavers. Lateral radiographs were obtained with the limb in various degrees of hip and knee flexion. The degree of axial shortening and bending of the stent were estimated by planimetry and used for in vitro fatigue testing. In contrast to our fatigue test method, the stents were mounted in elastic silicone tubing, bathed in phosphate buffered saline at 37°±2°C, and examined for fracture after 10 million cycles of chronic deformation. For unstented arteries, the distal SFA/proximal popliteal artery had the greatest axial compression (23%) versus the middle SFA (9%) or popliteal artery (14%) at 90°/90° knee/hip flexion. For stented arteries, the popliteal artery exhibited the most axial compression (11%) versus the middle SFA (3%) or distal SFA/proximal popliteal artery (6%) at 90°/90° knee/hip flexion. Axial compression of the stented popliteal artery at 70°/20° knee/hip flexion was 6%, with a deflection angle of 33°. Based on these parameters, chronic in vitro fatigue testing produced a range of responses in commercially available stents. Chronic 5% axial compression resulted in high rates of fracture in Luminexx (80%) and LifeStent (50%), with lower fracture rates for Absolute (3%), Protégé EverFlex (0%), and Smart (0%). Chronic 48° bending deformation resulted in high rates of fracture in Protégé EverFlex (100%), Smart (100%), and Luminexx (100%), with lower rates in Absolute (3%) and LifeStent (0%). Even with lower bending angle (70°), higher compression rate (40%), and an additional torsion component (180°, 90° clockwise), our fatigue data match Nikanorv's result for bending and torsion for Smart, Absolute, Luminexx, and Lifestent. This observation indicates that commercially available stents exhibit a variable ability to withstand chronic deformation in vitro, and their response is highly dependent on the type of deformation applied.

In addition, we used computer-based analysis to predict high strain areas during stent movement (bending, compression, torsion). Our FEA findings match our mechanical fatigue test results except for the Absolute (compression and torsion) and Smart (torsion) stents. Early fractures appeared with these stents (in contrast to the FEA findings, which indicated no high strain areas). An explanation for this mismatch might be the small number of test samples. Nevertheless, from our computer-simulated analysis of bending and axial compression, it was clear that the strain was concentrated in the zigzag unit with the bridge (Fig. 4D1). In the mechanical fatigue bending test, fractures were also observed at these points (Fig. 4D2). With the Smart stent, the strain was concentrated at the S-shaped bridges between the struts (Fig. 4E). The actual fractures (Fig. 4F) in the Smart stents were observed at that point in the mechanical fatigue test as well, which supports the authenticity of the data. The fractures observed near the bridge in bending and axial compression conditions had a higher risk of stent separation owing to loss of axial stent integrity, i.e., type 3 fracture.[16] Therefore, it seems that bending and axial compression could impart more critical stress to the stent than torsion.

With respect to design, a stent without the bridge on which the strain concentrates would likely survive without failure because dynamic loads are distributed equally to all struts. As a result, Misago could be expected to have a reduced risk of complete transverse fracture since it does not have the connections or bridges found in other stent designs. Optimizing stent link design would aid in the development of a dedicated stent for the popliteal artery, where the devices are subjected to a more severe bending and/or axial compression load than in the SFA.

Limitations

We are unaware of other reports utilizing FEA for evaluating stent design during simulated movement (stress), but other computer programs used to undertake similar evaluations may produce different results. However, our study should be seen as only an attempt to gain insight into the connection between stent design and the potential for fracture in vivo.

There are other limitations associated with the design and construction of our ex vivo setting: a larger angle for bending, evaluating longer stent lengths, and stents not implanted into a tube or another medium that mimics an in vivo situation. Finally, the fatigue tests

were performed under non-standardized conditions because these standardized methods do not exist. Another shortcoming was the small sample size for mechanical tests. There was also no consideration of material property or surface finish.

To our knowledge, pulsatile durability testing is standardized only by the American Society for Testing and Materials, but no industry standard for in vitro stent fracture fatigue testing in the SFA exists; although it may be difficult to reproduce the dynamics of the SFA, it is imperative that improved standards should be developed in all aspects of nitinol stent processing and testing to better identify the failure modes of SFA stenting. Physicians should apply some pressure on the medical device industry to standardize testing of stents and endoprostheses before marketing approval and clinical use.

In spite of these limitations, these simple tests offered a reproducible method of testing the differences in stent design; the acquired data gave us an indication of stent performance that might be expected in vivo. Even when the FEA results match those of the mechanical fatigue tests, the data have to be extrapolated with the greatest care before being applied to a clinical situation. Moreover, many stent strut structures are missed during even high resolution fluoroscopy, as we found in this study. Therefore, the currently reported low fracture rates with second-generation SFA stents should be interpreted cautiously.

Conclusion

The 7 nitinol SFA stents tested showed differences in the incidence of high strain zones that indicate the potential for stent fracture, which can be revealed only by functional investigation. Differences in stent design may play a major role in the occurrence of restenosis and reocclusion related to stent strut fractures. Mechanical bending has to be considered in future studies to assess the influence of differences in stent design, material, or even postinterventional drug treatment on the long-term patency of stents and endoprostheses in the femoropopliteal segment.

REFERENCES

1. Grimm J, Müller-Hülsbeck S, Jahnke T, et al. Randomized study to compare PTA alone versus PTA with Palmaz stent placement for femoropopliteal lesions. *J Vasc Interv Radiol*. 2001;12:935–942.
2. Krankenberg H, Schlüter M, Steinkamp HJ, et al. Nitinol stent implantation versus percutaneous transluminal angioplasty in superficial femoral artery lesions up to 10 cm in length: the femoral artery stenting trial (FAST). *Circulation*. 2007;116:285–292.
3. Schillinger M, Sabeti S, Loewe C, et al. Balloon angioplasty versus implantation of nitinol stents in the superficial femoral artery. *N Engl J Med*. 2006;354:1879–1888.
4. Duda SH, Pusich B, Richter G, et al. Sirolimus-eluting stents for the treatment of obstructive superficial femoral artery disease: six-month results. *Circulation*. 2002;106:1505–1509.
5. Duda SH, Bosiers M, Lammer J, et al. Sirolimus-eluting versus bare nitinol stent for obstructive superficial femoral artery disease: the SIROCCO II trial. *J Vasc Interv Radiol*. 2005;16:331–338.
6. Schlager O, Dick P, Sabeti S, et al. Long-segment SFA stenting—the dark sides: in-stent restenosis, clinical deterioration, and stent fractures. *J Endovasc Ther*. 2005;12:676–684.
7. Schulte KL, Müller-Hülsbeck S, Cao P, et al. MISAGO 1: first-in-man clinical trial with Misago nitinol stent. *EuroIntervention*. 2010;5:687–691.
8. Scheinert D, Scheinert S, Sax J, et al. Prevalence and clinical impact of stent fractures after femoropopliteal stenting. *J Am Coll Cardiol*. 2005;45:312–315.
9. Klein AJ, Chen SJ, Messenger JC, et al. Quantitative assessment of the conformational change in the femoropopliteal artery with leg movement. *Catheter Cardiovasc Interv*. 2009;74:787–798.
10. Cheng CP, Wilson NM, Hallett RL, et al. In vivo MR angiographic quantification of axial and twisting deformations of the superficial femoral artery resulting from maximum hip and knee flexion. *J Vasc Interv Radiol*. 2006;17:979–987.
11. Cheng CP, Choi G, Herfkens RJ, et al. The effect of aging on deformations of the superficial femoral artery resulting from hip and knee flexion: potential clinical implications. *J Vasc Interv Radiol*. 2010;21:195–202.
12. Brown R, Nguyen TD, Spincemaille P, et al. In vivo quantification of femoral-popliteal compression during isometric thigh contraction: assessment using MR angiography. *J Magn Reson Imaging*. 2009;29:1116–1124.

13. Dension A. Axial and bending fatigue resistance of nitinol stents. Proceedings of the International Conference on Shape Memory and Superelastic Technologies, Baden-Baden, Germany. 2004 Oct:95–102.

14. Bosiers M, Torsello G, Gissler HM, et al. Nitinol stent implantation in long superficial femoral artery lesions: 12-month results of the DURABIL-ITY I study. *J Endovasc Ther*. 2009;16:261–269.

15. Nikanorov A, Smouse HB, Osman K, et al. Fracture of self-expanding nitinol stents stressed in vitro under simulated intravascular conditions. *Vasc Surg*. 2008;48:435–340.

16. Jaff M, Dake M, Pompa J, et al. Standardized evaluation and reporting of stent fractures in clinical trials of noncoronary devices. *Catheter Cardiovasc Interv*. 2007;70: 460–462.